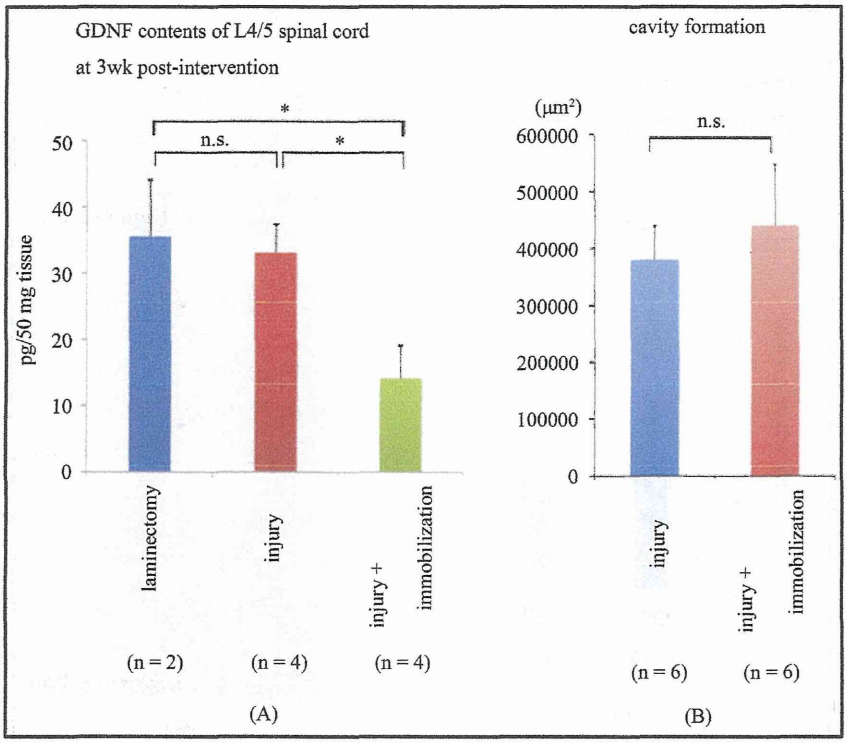


**Figure 2.** (A) ELISA for GDNF content of L4/5 spinal cord at 3 weeks postintervention; (B) Histogram showing the mean (±SD) cavity volume in the injury and injury + immobilization groups ($^{*}P < 0.05$, n.s.; not significant).

## 4. Discussion

Widenfalk *et al.* created the thoracic contusion model, using the NYU impactor in the same way as our contusion model and at the same thoracic level [23]. They presented the expression of GFR$\alpha$1 and RET in lumbar MNs of normal rats or rats with thoracic spinal cord injury. They also revealed no expression of GDNF in the lumbar segment of either normal or injured spinal cord. Their findings show that lumbar GDNF proteins are transported in both anterograde and retrograde directions from the spinal cord or muscle.

In this study, we have demonstrated that disuse muscle atrophy within the context of spinal cord injury exacerbates the reduction in GDNF proteins in caudal regions remote from the injury. The injury + immobilization group had lower GDNF levels in muscles and L4/5 spinal cord compared to the injury group [11]. While the injury + immobilization group had no significant difference from the injury group in the extent of spinal lesions. These data indicate that the decrease of GDNF in atrophic muscle cause the decrease in L4/5 spinal cord. Then we investigated whether the administration of recombinant GDNF proteins into the gastrocnemius muscle in the injury + immobilization group rescued $\alpha$-MN degeneration.

Figure 3 present that $\alpha$-MN degeneration was partially rescued by exogenous GDNF proteins into disuse muscle. These findings suggest that the depletion of GDNF protein by muscle atrophy causes a reduction in GDNF proteins at the L4/5 spinal cord segment. It is possible that in addition to exerting an effect through retrograde transport, GDNF affected $\alpha$-MN survival by being transported through the systemic circulation as well.

In this study, the mean volume of cavities around the lesion did not differ significantly between the injury and injury + immobilization group (Figure 2(B)). It was suggested that disuse muscle atrophy did not alter the extent of lesion. The injection of GDNF proteins into the gastrocnemius muscle partially rescued $\alpha$-MN degeneration in the L4/5 spinal cord segment. While the cavity volumes did not differ significantly between the PBS and GDNF injection group (Figure 3(C)). GDNF cause cell survival in the contused spinal cord tissues [24] [25]. Therefore the timing or volumes of GDNF injection may be late or insufficient respectively to prevent secondary effect of spinal cord injury.

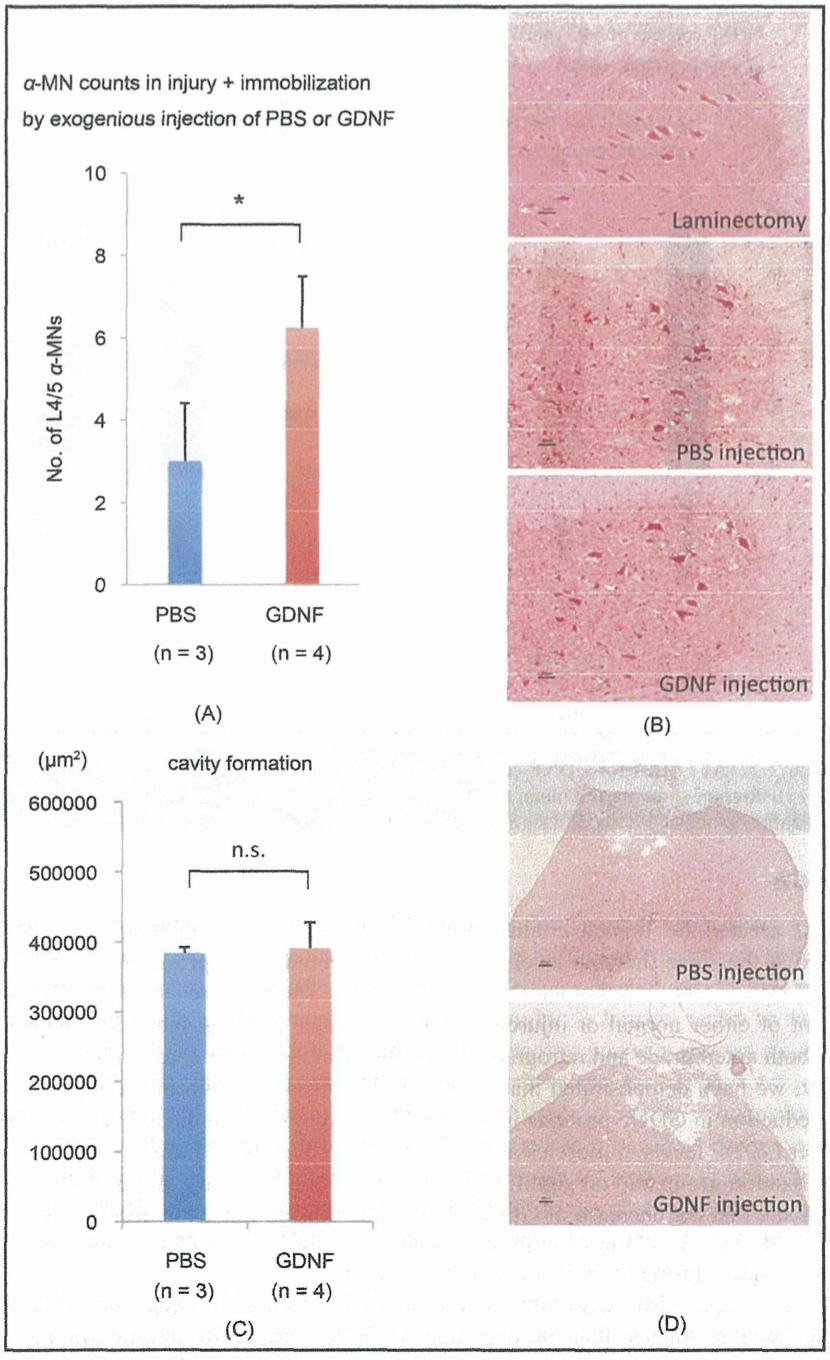


**Figure 3.** (A) α-MN counts in the injury + immobilization group by exogenous injection of recombinant rat GDNF or PBS into the gastrocnemius muscle; (B) HE staining of ventral horn at L4/5 segment in the Laminectomy, PBS injection and GDNF injection group. Black bar = 50 μm; (C) Histogram showing the mean (±SD) cavity volume in the PBS and GDNF injection groups; (D) HE staining of cavity lesions around epicenter. Black bar = 100 μm ass screws; (B) C2 pedicle screws.

## 5. Conclusion

Our findings suggest that the depletion of GDNF protein by muscle atrophy exacerbates MN degeneration in

caudal regions remote from the injury.

## Acknowledgements

This study was supported by grants from the Funding Program for World-Leading. Innovative R & D on Science and Technology and Global COE Program from the Japanese Ministry of Education, Culture, Sports, Science, and Technology. We thank Y. Takahashi for secretarial aid.

## Conflict of Interest Declaration

The authors declare no conflicts of interest with respect to the authorship or publication of this article.

## References

[1] Bohn, M.C. (2004) Motoneurons Crave Glial Cell Line-Derived Neurotrophic Factor. *Experimental Neurology*, **190**, 263-275. http://dx.doi.org/10.1016/j.expneurol.2004.08.012

[2] Airaksinen, M.S. and Saarma, M. (2002) The GDNF Family: Signalling, Biological Functions and Therapeutic Value. *Nature Reviews Neuroscience*, **3**, 383-394. http://dx.doi.org/10.1038/nrn812

[3] Cary, G.A. and La Spada, A.R. (2008) Androgen Receptor Function in Motor Neuron Survival and Degeneration. *Physical Medicine and Rehabilitation Clinics of North America*, **19**, 479-494. http://dx.doi.org/10.1016/j.pmr.2008.03.002

[4] Kablar, B. and Rudnicki, M.A. (1999) Development in the Absence of Skeletal Muscle Results in the Sequential Ablation of Motor Neurons from the Spinal Cord to the Brain. *Developmental Biology*, **208**, 93-109. http://dx.doi.org/10.1006/dbio.1998.9184

[5] Korsching, S. (1993) The Neurotrophic Factor Concept: A Reexamination. *The Journal of Neuroscience*, **13**, 2739-2748.

[6] Booth, F.W. (1982) Effect of Limb Immobilization on Skeletal Muscle. *Journal of Applied Physiology: Respiratory, Environmental and Exercise Physiology*, **52**, 1113-1118.

[7] Glover, E.I., Phillips, S.M., Oates, B.R., Tang, J.E., Tarnopolsky, M.A., Selby, A., Smith, K. and Rennie, M.J. (2008) Immobilization Induces Anabolic Resistance in Human Myofibrillar Protein Synthesis with Low and High Dose Amino Acid Infusion. *The Journal of Physiology*, **586**, 6049-6061. http://dx.doi.org/10.1113/jphysiol.2008.160333

[8] Murton, A.J. and Greenhaff, P.L. (2009) Muscle Atrophy in Immobilization and Senescence in Humans. *Current Opinion in Neurology*, **22**, 500-505. http://dx.doi.org/10.1097/WCO.0b013e32832f15e1

[9] Gallego, R., Kuno, M., Núñez, R. and Snider, W.D. (1979) Dependence of Motoneurone Properties on the Length of Immobilized Muscle. *The Journal of Physiology*, **291**, 179-189.

[10] Gomes, A.R., Cornachione, A., Salvini, T.F. and Mattiello-Sverzut, A.C. (2007) Morphological Effects of Two Protocols of Passive Stretch over the Immobilized Rat Soleus Muscle. *Journal of Anatomy*, **210**, 328-335. http://dx.doi.org/10.1111/j.1469-7580.2007.00697.x

[11] Ohnishi, Y., Iwatsuki, K., Shinzawa, K., Nakai, Y., Ishihara, M. and Yoshimine, T. (2012) Disuse Muscle Atrophy Exacerbates Motor Neuronal Degeneration Caudal to the Site of Spinal Cord Injury. *NeuroReport*, **23**, 157-161. http://dx.doi.org/10.1097/WNR.0b013e32834f4048

[12] Côté, M.P., Azzam, G.A., Lemay, M.A., Zhukareva, V. and Houlé, J.D. (2011) Activity-Dependent Increase in Neurotrophic Factors Is Associated with an Enhanced Modulation of Spinal Reflexes after Spinal Cord Injury. *Journal of Neurotrauma*, **28**, 299-309. http://dx.doi.org/10.1089/neu.2010.1594

[13] Wehrwein, E.A., Roskelley, E.M. and Spitsbergen, J.M. (2002) GDNF Is Regulated in an Activity-Dependent Manner in Rat Skeletal Muscle. *Muscle & Nerve*, **26**, 206-211. http://dx.doi.org/10.1002/mus.10179

[14] Aoki, M., Kishima, H., Yoshimura, K., Ishihara, M., Ueno, M., Hata, K., Yamashita, T., Iwatsuki, K. and Yoshimine, T. (2010) Limited Functional Recovery in Rats with Complete Spinal Cord Injury after Transplantation of Whole-Layer Olfactory Mucosa: Laboratory Investigation. *Journal of Neurosurgery: Spine*, **12**, 122-130. http://dx.doi.org/10.3171/2009.9.SPINE09233

[15] Ide, C., Nakai, Y., Nakano, N., Seo, T.B., Yamada, Y., Endo, K., Noda, T., Saito, F., Suzuki, Y., Fukushima, M. and Nakatani, T. (2010) Bone Marrow Stromal Cell Transplantation for Treatment of Sub-Acute Spinal Cord Injury in the Rat. *Brain Research*, **1332**, 32-47. http://dx.doi.org/10.1016/j.brainres.2010.03.043

[16] Iwatsuki, K., Yoshimine, T., Kishima, H., Aoki, M., Yoshimura, K., Ishihara, M., Ohnishi, Y. and Lima, C. (2008) Transplantation of Olfactory Mucosa Following Spinal Cord Injury Promotes Recovery in Rats. *NeuroReport*, **19**, 1249-1252. http://dx.doi.org/10.1097/WNR.0b013e328305b70b

[17] Gruner, J.A. (1992) A Monitored Contusion Model of Spinal Cord Injury in the Rat. *Journal of Neurotrauma*, **9**, 123-128. http://dx.doi.org/10.1089/neu.1992.9.123

[18] Metz, G.A., Curt, A., van de Meent, H., Klusman, I., Schwab, M.E. and Dietz, V. (2000) Validation of the Weight-Drop Contusion Model in Rats: A Comparative Study of Human Spinal Cord Injury. *Journal of Neurotrauma*, **17**, 1-17. http://dx.doi.org/10.1089/neu.2000.17.1

[19] Young, W. (2002) Spinal Cord Contusion Models. *Progress in Brain Research*, **137**, 231-255. http://dx.doi.org/10.1016/S0079-6123(02)37019-5

[20] Ichiyama, R.M., Broman, J., Edgerton, V.R. and Havton, L.A. (2006) Ultrastructural Synaptic Features Differ between Alpha- and Gamma-Motoneurons Innervating the Tibialis Anterior Muscle in the Rat. *Journal of Comparative Neurology*, **499**, 306-315. http://dx.doi.org/10.1002/cne.21110

[21] Ishihara, A., Ohira, Y., Tanaka, M., Nishikawa, W., Ishioka, N., Higashibata, A., Izumi, R., Shimazu, T. and Ibata, Y. (2001) Cell Body Size and Succinate Dehydrogenase Activity of Spinal Motoneurons Innervating the Soleus Muscle in Mice, Rats, and Cats. *Neurochemical Research*, **26**, 1301-1304. http://dx.doi.org/10.1023/A:1014245417017

[22] Roland, R.R., Matsumoto, A., Zhong, H., Ishihara, A. and Edgerton, V.R. (2007) Rat $\alpha$- and $\gamma$-Motoneuron Soma Size and Succinate Dehydrogenase Activity Are Independent of Neuromuscular Activity Level. *Muscle & Nerve*, **36**, 234-241. http://dx.doi.org/10.1002/mus.20810

[23] Widenfalk, J., Lundströmer, K., Jubran, M., Brene, S. and Olson, L. (2001) Neurotrophic Factors and Receptors in the Immature and Adult Spinal Cord after Mechanical Injury or Kainic Acid. *The Journal of Neuroscience*, **21**, 3457-3475.

[24] Iannotti, C., Zhang, Y.P., Shields, C.B., Han, Y., Burke, D.A. and Xu, X.M. (2004) A Neuroprotective Role of Glial Cell Line-Derived Neurotrophic Factor Following Moderate Spinal Cord Contusion Injury. *Experimental Neurology*, **189**, 317-332. http://dx.doi.org/10.1016/j.expneurol.2004.05.033

[25] Tai, M.H., Cheng, H., Wu, J.P., Liu, Y.L., Lin, P.R., Kuo, J.S., Tseng, C.J. and Tzeng, S.F. (2003) Gene Transfer of Glial Cell Line-Derived Neurotrophic Factor Promotes Functional Recovery Following Spinal Cord Contusion. *Experimental Neurology*, **183**, 508-515. http://dx.doi.org/10.1016/S0014-4886(03)00130-4

Journal of Neuroscience Research 00:00–00 (2015)

# Olfactory Sphere Cells Are a Cell Source for γ-Aminobutyric Acid-Producing Neurons

Yu-ichiro Ohnishi,[1]* Tomoyuki Maruo,[1] Koei Shinzawa,[2] Koichi Iwatsuki,[1] Takashi Moriwaki,[1] Satoru Oshino,[1,3] Haruhiko Kishima,[1,3] and Toshiki Yoshimine[1]

[1]Department of Neurosurgery, Osaka University Medical School, Suita, Osaka, Japan
[2]Department of Molecular Genetics, Osaka University Medical School, Suita, Osaka, Japan
[3]Epilepsy Center, Osaka University Hospital, Suita, Osaka, Japan

Olfactory sphere cells (OSCs) are stem cells generated by culturing olfactory mucosa. Adult rat OSCs express oligodendrocyte progenitor cell (OPC) markers and differentiate into mature oligodendrocytes. Although OSCs also express nestin, a marker of neural stem cells (NSCs), it remains unclear whether adult rat OSCs are multipotent and capable of giving rise to neurons as well as oligodendrocytes. Valproic acid (VPA) is a histone deacetylase inhibitor that has the contradictory capacity to induce both differentiation of NSCs and dedifferentiation of OPCs. This study investigates a potential role for VPA in inducing either differentiation or dedifferentiation of adult rat OSCs. Treatment of OSCs with VPA induced hyperacetylation of histones and decreased cell proliferation in the absence of changes in the number of nestin-positive cells. Furthermore, VPA promoted the genesis of γ-aminobutyric acid (GABA)-producing neurons identified by expression of Tuj1/GAD67/GABA while repressing oligodendrocyte production. These findings suggest that OSCs treated with VPA did not exhibit stem cell properties indicative of dedifferentiation but rather switched to a neuronal identity during their terminal differentiation. OSCs were then transplanted into the hippocampus of rats with kainic acid-induced temporal lobe epilepsy and were systemically given VPA. Although grafted OSCs expressed Tuj1 and GAD67, these cells did not sufficiently inhibit epileptic activity. These results suggest that OSCs are a transplantable cell source for GABA-producing neurons that can be modulated by VPA. However, further investigation is required to develop them for clinical applications. 

**Key words:** GABA; histone deacetylase; oligodendrocyte progenitor; olfactory sphere

Olfactory spheres (OSs) are clusters of cells generated by culturing olfactory mucosa and consist of cells expressing markers of neural stem cells (NSCs), glial cells, and neurons (Murrell et al., 2005; Othman et al., 2005; Murdoch and Roskams, 2008; Tome et al., 2009). Various culture conditions generate OSs that differ according to species and developmental stage. It has been reported that these different OSs have different progenitors or stem cell characteristics (Zhang et al., 2004; Murrell et al., 2005; Barraud et al., 2007; Murdoch and Roskams, 2008; Tome et al., 2009; Krolewski et al., 2011; Lindsay et al., 2013).

We previously reported that adult rat OS cells (OSCs) express predominantly oligodendrocyte progenitor cell (OPC) markers (e.g., NG2, PFGFRα, Olig2, A2B5) and that transplanted OSCs differentiate into oligodendrocytes following spinal cord injury and into Schwann cells after peripheral nerve injury (Ohnishi et al., 2013). Under standard culture conditions, OSCs rarely differentiate into neurons. Although OSs weakly expressed Tuj1 and glial fibrillary acidic protein (GFAP) in differentiation cultures, these Tuj1- and GFAP-positive cells did not resemble bona fide neurons and astrocytes morphologically. Adult rat OSCs also express nestin, a marker of NSCs, which suggests that the OSCs might be multipotent cells that can give rise to neurons as well as to oligodendrocytes in response to different environmental and pharmacologic cues.

In addition, there are some reports that OPCs might also give rise to neurons in certain contexts. For instance, OPCs express nestin protein, which decreases over the course of oligodendrocyte development (Gallo and Armstrong, 1995; Belachew et al., 2003). Although OPCs do not generate neurons under normal physiological conditions (Richardson et al., 2011), OPCs from postnatal rat optic nerves could be reprogrammed to a neuronal fate (Kondo and Raff, 2000). NG2-expressing cells residing in

Contract grant sponsor: Grant-in-Aid for Scientists (C). Grant Number: 25462215

*Correspondence to: Yu-ichiro Ohnishi, MD, PhD, Department of Neurosurgery, Osaka University Medical School, 2-2 Yamadaoka, Suita, Osaka 565-0871, Japan. E-mail: ohnishi@nsurg.med.osaka-u.ac.jp

Received 26 November 2014; Revised 10 February 2015; Accepted 18 February 2015

**Published online 00 Month 2015 in Wiley Online Library (wileyonlinelibrary.com). DOI: 10.1002/jnr.23585**

the postnatal CNS are considered OPCs, and it has been reported that early postnatal NG2 cells are multipotent and generate γ-aminobutyric acid (GABA)-ergic neurons (Belachew et al., 2003). However, the stem cell potential of adult OPCs (i.e., NG2 cells) has not been fully explored in normal physiologic conditions or in response to molecular and chemical agents that are known to modulate cell fate potential.

Valproic acid (VPA) is a histone deacetylase (HDAC) inhibitor used clinically as an anticonvulsant and treatment for epilepsy. VPA functions as an HDAC inhibitor and is thus able to induce cell cycle arrest, senescence, and differentiation (Gottlicher et al., 2001; Gurvich et al., 2004; Balasubramaniyan et al., 2006). VPA has been shown to promote the specification of neurons from adult NSCs of the hippocampal dentate gyrus (Hsieh et al., 2004). HDACs are also a necessary component of the oligodendrocyte differentiation program (Marin-Husstege et al., 2002; Conway et al., 2012), and HDAC inhibitors induce dedifferentiation of OPCs (Lyssiotis et al., 2007).

The present study investigates whether VPA induces dedifferentiation of adult rat OSCs and/or promotes their differentiation into neurons. We found that VPA promoted differentiation into GABA-producing neurons at the expense of oligodendrocytes but did not find compelling evidence of dedifferentiation of OSCs into nestin-expressing NSCs. We then determined that transplantation of OSCs into the hippocampus of rats with kainic acid (KA) induced temporal lobe epilepsy (TLE), which, followed by systemic treatment with VPA, promoted the generation of inhibitory neurons.

## MATERIALS AND METHODS

### Animals

Eight-week-old male Sprague-Dawley rats (wild type, n = 36; transgenic SD-Tg rats, n = 8) were obtained from Japan SLC (Hamamatsu, Japan). These transgenic rats express the enhanced green fluorescent protein (EGFP) gene under the control of a ubiquitously expressed chicken β-actin (CAG) promoter. All procedures were performed in accordance with the guidelines of the Laboratory Animals Care and Use Committee of the Osaka University Faculty of Medicine. Every effort was made to minimize the number of animals used and to limit their suffering.

### OS Culture

OSs were generated as reported elsewhere (Ohnishi et al., 2013). In brief, the olfactory mucosa was located in the caudal part of the septum and identified by its yellowish color. Tissue was carefully microdissected from each side of the septum to avoid contamination by other tissues, such as the olfactory bulb or the cribriform plate. The mucosa was dissociated mechanically and then treated for 60 min at 37°C with an enzyme solution consisting of collagenase (Wako, Osaka, Japan), dispase (Sanko Junyaku, Tokyo, Japan), DNase I (Sigma-Aldrich, St Louis, MO), and hyaluronidase (Sigma-Aldrich) in Dulbecco's modified Eagle's medium/F12 medium (DF; Invitrogen, Carlsbad, CA). Culture dishes were coated with poly(2-hydroxyethyl methacrylate; P3932; Sigma-Aldrich) to prevent attachment of cells to the bottom of the dish. Dissociated cells ($1 \times 10^6$/ml) were plated onto poly(2-hydroxyethyl methacrylate)-coated dishes in DF medium containing B27 supplement (Invitrogen), 20 ng/ml basic fibroblast growth factor (bFGF; Sigma-Aldrich), 20 ng/ml epidermal growth factor (EGF; Sigma-Aldrich), 5 μg/ml heparin (Sigma-Aldrich), and antibiotic–antimycotic (15240; Invitrogen). Cultures were incubated at 37°C in a 5% $CO_2$ atmosphere, and the medium was changed every 2–3 days. Cell clusters were classified as OSs if they were spherical in shape and had a diameter of at least 50 μm.

### Differentiation Culture

After 8 days in culture, OSs were treated with trypsin-EDTA (Invitrogen), plated onto poly-L-lysine-coated four-well chamber slides (Becton Dickinson, Franklin Lakes, NJ) at approximately $1 \times 10^3$ cells per well, and cultured for 7 days in DF medium supplemented with $N_2$ (Invitrogen), B27, 20 ng/ml bFGF, 20 ng/ml EGF, and antibiotic–antimycotic solution with 0, 0.3, and 1 mM VPA (Sigma-Aldrich).

### Immunocytochemistry

OSCs were fixed with 4% paraformaldehyde (PFA), incubated for 1 hr at room temperature in blocking solution, incubated overnight at 4°C with the primary antibody, washed, and incubated overnight at 4°C in the appropriate species-directed secondary antibody. The primary antibodies were anti-β3-tubulin (Tuj1; 1:200 mouse monoclonal antibody; Abcam, Cambridge, United Kingdom; or 1:200 rabbit polyclonal antibody; Abcam), anti-GFAP (1:300 mouse monoclonal antibody; Cell Signaling Technology, Danvers, MA), antireceptor-interacting protein (RIP; 1:100 rabbit monoclonal antibody; Cell Signaling Technology), antiacetyl-histone H4 (Lys8; 1:100 rabbit polyclonal antibody; AcH4K8; Cell Signaling Technology), antiglutamic acid decarboxylase 67 (GAD67; 1:200 mouse monoclonal antibody; Millipore, Billerica, MA), anti-GABA (1:5,000 rabbit monoclonal antibody; Sigma-Aldrich), anti-MAP2 (1:200 rabbit polyclonal; Abcam), anti-O4 (1:200 mouse monoclonal; Neuromics, Edina, MN), and anti-5-bromo-2-deoxy-uridine (BrdU) antibodies (BrdU labeling and detection kit II; catalog No. 1 299 964; Roche, Indianapolis, IN). BrdU labeling was detected with a kit containing the Boehringer-Mannheim monoclonal antibody BMG6H8 directed against BrdU (1:10 mouse BrdU labeling and detection kit II; Roche).

The secondary antibodies used were DyLight 488-conjugated goat anti-mouse (1:200; Kirkegaard and Perry Laboratories, Gaithersburg, MD) or DyLight 549-conjugated goat anti-rabbit (1:200; Kirkegaard and Perry Laboratories). To visualize cell nuclei, slides were then counterstained with 4′,6-diamidino-2-phenylindole dihydrochloride (DAPI; Vector Laboratories, Burlingame, CA). Cell phenotype assessments and cell counts were obtained from images captured with a confocal laser fluorescence microscope (FV-1000D; Olympus, Tokyo, Japan). The percentages of Tuj1-, RIP-, GAD67-, GABA-, AcH4K8-, MAP2-, O4-, and GFAP-positive cells are shown as mean ± SD of three images from three independent experiments. Primary and secondary antibodies are listed in Table I.

**TABLE I. Antibodies Used in This Study**

| Primary antibodies | Target | Host | Code/clone | Dilution |
|---|---|---|---|---|
| AcH3 | Acetyl-histone H3 | Rabbit | DAM1823380 | 1/1,000 |
| AcH4 | Acetyl-histone H4 | Rabbit | DAM1770301 | 1/1,000 |
| AcH4K8 | Acetyl-histone H4 (Lys8) | Rabbit | No. 2594 | 1/100 |
| BrdU | Mitosis | Mouse | BMG6H8 | 1/10 |
| Calbindin | GABAergic neurons | Rabbit | ab11426 | 1/500 |
| GABA | GABAergic neurons | Rabbit | A2052 | 1/5,000 |
| GFAP | Astrocytes | Mouse | ab10062 | 1/250 |
| EGFP | GFP | Goat | ab5450 | 1/500 |
| GAD67 | GABAergic neurons | Mouse | MAB5406 | 1/5,000 1/500 |
| H3 | Histone H3 | Rabbit | DAM1785852 | 1/1,000 |
| H4 | Histone H4 | Rabbit | DAM1557154 | 1/1,000 |
| MAP2 | Neurons | Rabbit | ab32454 | 1/200 |
| O4 | Oligodendrocytes | Mouse | MO15002 | 1/200 |
| RIP | Oligodendrocytes | Rabbit | D94C12 | 1/100 |
| Tubulin | α-Tubulin | Mouse | ab7291 | 1/1,000 |
| Tuj1 | Neurons | Mouse | ab14545 | 1/200 |
| Tuj1 | Neurons | Rabbit | ab18207 | 1/200 |

### Western Blotting

Histones were acid extracted from OSCs supplemented with trichostatin A (Sigma-Aldrich) as described by Shechter et al. (2007), and the extracts were boiled in SDS sample buffer (62.5 mM Tris-HCl, pH 6.8 [Nippon Gene, Tokyo, Japan]), 2% SDS (Nippon Gene), 10% glycerol (Sigma-Aldrich), and 50 mM DTT (Wako, Osaka, Japan) with trichostatin A. Total protein was extracted from OSCs in extraction buffer (10 mM Tris-HCl [Nippon Gene], pH 7.4, 0.1% SDS [Nippon Gene], 1% Triton X [Sigma-Aldrich], and 100 mM NaCl [Wako]) supplemented with protease inhibitors (Halt protease inhibitor cocktail; Thermo Scientific, Rockford, IL) and phenylmethanesulfonyl fluoride (Sigma-Aldrich). Protein concentrations were measured with a Qubit protein assay kit (Invitrogen) after microcentrifugation.

Samples were resolved by electrophoresis with NuPAGE Novex 4–12% Bis-Tris gels (Invitrogen) and transferred to polyvinylidene fluoride membranes (Invitrogen). Blots were blocked with 5% ECL blocking agent (GE Healthcare Life Sciences, Piscataway, NJ) in Tris-buffered saline (Nippon Gene) with Triton X-100 (TBST) for 1 hr and then incubated with the primary antibody in TBST overnight at 4°C. The primary antibodies used were rabbit antihistone H3 antibody (1:1,000; Millipore), rabbit antihistone H4 antibody (1:1,000; Millipore), rabbit antiacetylated (Ac)-histone H3 antibody (1:1,000; Millipore), rabbit anti-Ac-histone H4 antibody (1:1,000; Millipore), anti-GAD67 (1:5,000 mouse monoclonal antibody; Millipore), and anti-α-tubulin (1:1,000 rabbit polyclonal antibody; Abcam). After having been washed with TBST, membranes were incubated with horseradish peroxidase-conjugated anti-rabbit (1:2,000; Cell Signaling Technology) or horseradish peroxidase-conjugated anti-mouse secondary antibody (1:50,000; GE Healthcare Life Sciences) for 1 hr at room temperature. Blots were washed again with TBST and developed with ECL Plus reagent (GE Healthcare Life Sciences). Signal intensities were determined in an IS-8000 FluorChem digital imaging system (Alpha Innotech, San Leandro, CA).

### RT-PCR

RNA was extracted from spheres harvested from differentiating cultures with commercially available kits (Qiagen, Hilden, Germany). Total RNA (1 μg) was reverse transcribed with the OneStep RT-PCR kit (Qiagen). The primers used and the size in base pairs (bp) of the expected amplicons were glyceraldehyde-3-phosphate dehydrogenase, CCTCTGGAAAGCTGTGGCGT (forward) and TTGGAGGCCATGTAGGCCAT (reverse), 430 bp; nestin, CAGGCTTCTCTTGGCTTTCTGG (forward) and TGGTGAGGGTTGAGGTTTGT (reverse), 431 bp. Reverse transcription was performed at 50°C for 30 min. PCR was performed at 94°C for 30 sec, 56°C for 40 sec, and 72°C for 50 sec. The number of PCR cycles performed was 35.

### Induction of Status Epilepticus

Five-week-old rats were treated with graded intraperitoneal injections of KA (Sigma-Aldrich; 3.0 mg/kg/hr) for 3–4 hr to induce status epilepticus (Rao et al., 2006, 2007). Motor seizures were characterized by unilateral forelimb clonus with lordotic posture (stage 3 seizures), bilateral forelimb clonus and rearing (stage 4 seizures), and bilateral forelimb clonus with rearing and falling (stage 5 seizures). All rats exhibited stage 5 seizures during the 4 hr of observation after the onset of status epilepticus. Motor seizures subsided gradually thereafter and were not apparent 12 hr after the onset of status epilepticus.

### Grafting of OSCs Into the Hippocampus of Epileptic Rats

Rats were placed under inhalation anesthesia with sevoflurane (2.5%; Maruishi Pharmaceutical, Osaka, Japan) and $O_2$. Five days after status epilepticus induction, cells were transplanted into rats with a Hamilton syringe connected to a microglass pipette with a stereotaxic injector (Narishige, Tokyo, Japan). Cells for transplantation were prepared from trypsinized sphere cells and diluted in DF medium to $1 \times 10^4$ cells/μl. The tip of the micropipette was inserted into each of two sites in every hippocampus at the following stereotaxic coordinates: 1)

anteroposterior (AP) = 3 mm from bregma, lateral (L) = 2 mm from midline, and ventral (V) = 3.5 mm from surface of the brain; 2) AP = 4 mm, L = 3 mm, V = 3.5 mm. A cell suspension control medium without cells with a volume of 2 μl was injected at a rate of 1 μl/min in the right or the left side. After injection, all rats received daily subcutaneous injections of gentamicin (8 mg/kg; Wako), and daily intraperitoneal injections of VPA (150 mg/kg; n = 6) or phosphate-buffered saline (PBS; n = 4) were administered for the following 7 days. To test the effect of transplanted OSCs on spontaneous seizures, we performed continuous electroencephalographic (EEG) monitoring in TLE model rats at 4 weeks after transplantation (PBS, n = 3; VPA, n = 4). Rat tissues were examined at 4-weeks posttransplantation (PBS, n = 4; VPA, n = 6).

Rats were anesthetized and tissues were fixed by transcardial perfusion with 100 ml PBS (Nippon Gene), followed by 4% PFA (Wako). Brains were embedded in optimal cutting temperature compound (Tissue Tek, Sakura Finetek, Tokyo, Japan), and 10-μm-thick sections were coronally cut from the blocks with a cryostat (CM1510S; Leica, Tokyo, Japan). Every tenth section was processed for immunostaining.

### Immunohistochemistry

Sections were stained with anti-GFP (1:500 goat polyclonal antibody; Abcam), anti-GAD67 (1:500 mouse monoclonal antibody; Millipore), anticalbindin (1:500 rabbit polyclonal antibody; Abcam), and anti-Tuj1 (1:200 mouse monoclonal antibody). The secondary antibodies used were DyLight 650-conjugated donkey anti-mouse antibody (1:1,000; Abcam), DyLight 594-conjugated donkey anti-rabbit antibody (1:1,000; Abcam), and DyLight 488-conjugated donkey anti-goat antibody (1:1,000; Abcam). Slides were counterstained with DAPI. Fluorescence images were captured with a confocal laser microscope (FV-1000D; Olympus, Tokyo, Japan). To determine the fate of transplanted cells, the number of GFP-positive cell counts and the percentage of GFP-positive cells colabeled with GAD67 and calbindin were determined by confocal microscopy. We chose and analyzed three hippocampal sections containing most transplanted cells for each animal. Three fields per chosen section were assessed by using a ×200 field. The GFP-positive cell counts were estimated by counting GFP-positive cells per field on digitized images.

The percentage of grafted cells that survived was estimated by counting all GFP-positive cells across 10 serial coronal sections spaced 100 μm apart. Quantifications of cell bodies stained with GFP were made from digitized images. The percentage of surviving cells was estimated as 100 × (number of survived cells)/(number of transplanted cells).

### Electrode Implantation

To record electrical activity in the brain, customized silver electrode needles (0.2 mm outer diameter; Unique Medical Co., Tokyo, Japan) were implanted laterally into the hippocampus of rats that had received VPA (n = 4) or PBS (n = 3). Burr holes were drilled 4 mm behind the bregma and 3 mm lateral from midline sutures. Electrodes were inserted into target regions (depth 3.5 mm) with an electrode manipulator. A common reference electrode was placed near the lambda. The entire implantation procedure was performed with animals under sevoflurane anesthesia (2–4% for induction, initiated at 3%; 0.5–2.0% for maintenance).

### EEG Recordings

Electrodes were implanted into rats that had received VPA (n = 4) or PBS (n = 3), and rats were continuously monitored by EEG recording. Electrical activity was recorded and analyzed in an EEG system (Nihon Koden, Tokyo, Japan). EEG data were collected with a sampling rate of 1,000 Hz and stored on a hard disk for offline analysis. The recordings were obtained with 0.3-Hz and 70-Hz low- and high-frequency filters. Epileptic spikes were recognized against background according to their large amplitude (more than threefold baseline amplitude). EEGs were recorded for 20 min after electrode implantation. A ratio describing the degree of decrease (decrease ratio) in epileptic spikes was determined by subtracting the number of spikes observed in the grafted hippocampus from the number in the vehicle hippocampus and dividing this value by the total number of spikes in the vehicle hippocampus.

### Statistical Analysis

Data were analyzed by one-way ANOVA. In the case of a significant F ratio, Tukey's post hoc test was performed. The level of significance was set at $P < 0.05$, and data are presented as mean ± SD unless otherwise indicated. Data were obtained from at least three independent experiments.

## RESULTS

### VPA Induced Differentiation of Adult Rat OSCs Into Neurons

OSCs express OPC markers and nestin and undergo oligodendrocyte differentiation (Ohnishi et al., 2013). We investigated whether VPA induced differentiation of rat OSCs into neurons or dedifferentiation of OSCs into NSCs. We hypothesized that, if OSCs are converted to a dedifferentiation state by VPA, treated OSCs would be capable of giving rise to all three neural lineages (astrocytes, neurons, and oligodendrocytes). We treated OSCs with 0, 0.3, or 1 mM VPA in culture and investigated the differentiation of OSCs by immunocytochemistry with antibodies against neuronal and oligocyte–glial markers. Immunofluorescence analysis of cell-type-specific immunohistochemistry (IHC) indicated that VPA significantly increased the frequency of Tuj1- and MAP2-positive neuronal cells in OSCs (Fig. 1A,D). The percentage of Tuj1-positive cells was 14.9% ± 13.4% (mean ± SD), 32.7% ± 16.4%, and 72.9% ± 16.8% at 0-, 0.3-, and 1-mM VPA treatment, respectively (Fig. 1B). By contrast, VPA significantly decreased the frequency of RIP- and O4-positive oligodendrocyte-lineage cells (Fig. 1A); the percentage of RIP-positive cells was 89.5% ± 10.7%, 70.2% ± 7.9%, and 9.4% ± 11.1% at 0-, 0.3-, and 1-mM VPA treatment, respectively (Fig. 1B). In contrast, the percentage of GFAP-positive cells (i.e., astroglia) was not significantly different, 3.4% ± 3.5%, 7.3% ± 1.8%, and

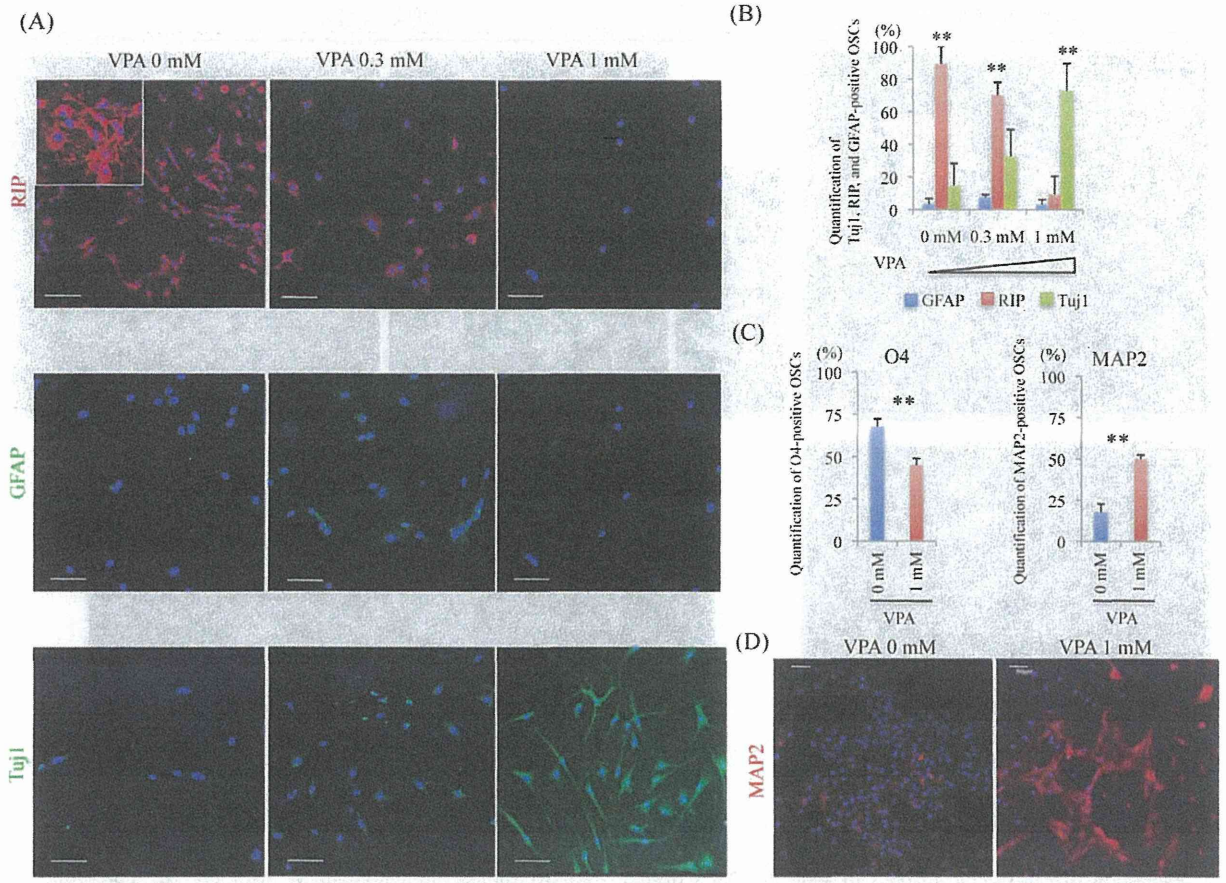


Fig. 1. VPA induced differentiation of adult rat OSCs into neurons. **A:** Immunocytochemistry for neuronal and glial markers in olfactory sphere cells cultured with 0, 0.3, or 1 mM VPA. Single-plane images of cells at high magnification are provided in **inset**. **B:** Quantification of Tuj1-, RIP-, and GFAP-positive OSCs. VPA increased the frequency of Tuj1-positive OSCs and decreased the frequency of RIP-positive OSCs. The number of GFAP-positive cells was not significantly different. **C:** Treatment with VPA resulted in an increase in the number of MAP2-positive cells and a decrease in the number O4-positive cells. **D:** Immunocytochemistry for MAP2 in OSCs cultured with 0 and 1 mM VPA. Blue: DAPI-labeled nuclei. Error bars indicate SD. $^{**}P < 0.01$. Scale bars = 50 μm. [Color figure can be viewed in the online issue, which is available at wileyonlinelibrary.com.]

3.1% ± 3.1% at 0-, 0.3-, and 1-mM-VPA treatment, respectively (Fig. 1A,B).

To determine whether OSCs coexpress neuronal and glial markers, we carried out double-labeling analysis of OSCs treated with 1 mM VPA or VPA-free control by immunocytochemistry. In control OSCs, some (less than 10%) Tuj1-positive OSCs were double positive for GFAP (Fig. 2A). In contrast, Tuj1-positive OSCs rarely coexpressed GFAP in 1-mM VPA-treated cells (Fig. 2C). In both control and 1-mM VPA-treated cells, O4-postive cells were almost never found to coexpress neurofilament (NF; Fig. 2B,D). Consistent with an oligodendrocyte identity, O4-positive cells exhibited a branched morphology (Fig. 2B). However, some (less than 10%) Tuj1-positive OSCs coexpressed RIP (Fig. 2E, left); these double-positive cells seemed to be undifferentiated or immature cells based on their simple, round morphology. Altogether, these findings indicate that VPA induced differentiation of adult rat OSCs into neurons at the expense of oligodendrocytes but did not affect astrogliogenesis.

To investigate the HDAC inhibitor activity of VPA, we quantified the levels of histone acetylation in OSCs. We treated cultured OSCs with VPA and harvested cell lysates from culture 7 days after the initiation of treatment. We then analyzed cell lysates by Western blotting with antibodies specific for total histone H3, total histone H4, acetylated histone H3, and acetylated histone H4. We also investigated the acetylation of histone H4 by immunocytochemistry with antibodies against histone H4 acetylation at lysine 8 (AcH4K8). AcH4K8 is known to correlate with chromatin remodeling activity and the regulation of gene expression (Fukuda et al., 2006). The levels of acetylated histones H3 and H4 increased following treatment with VPA in a dose-dependent manner (Fig. 3C). Similarly, the percentages of AcH4K8-positive cells were 9.2% ± 5.4%, 14.1% ± 5.7%, and 36.4% ± 16.0% at

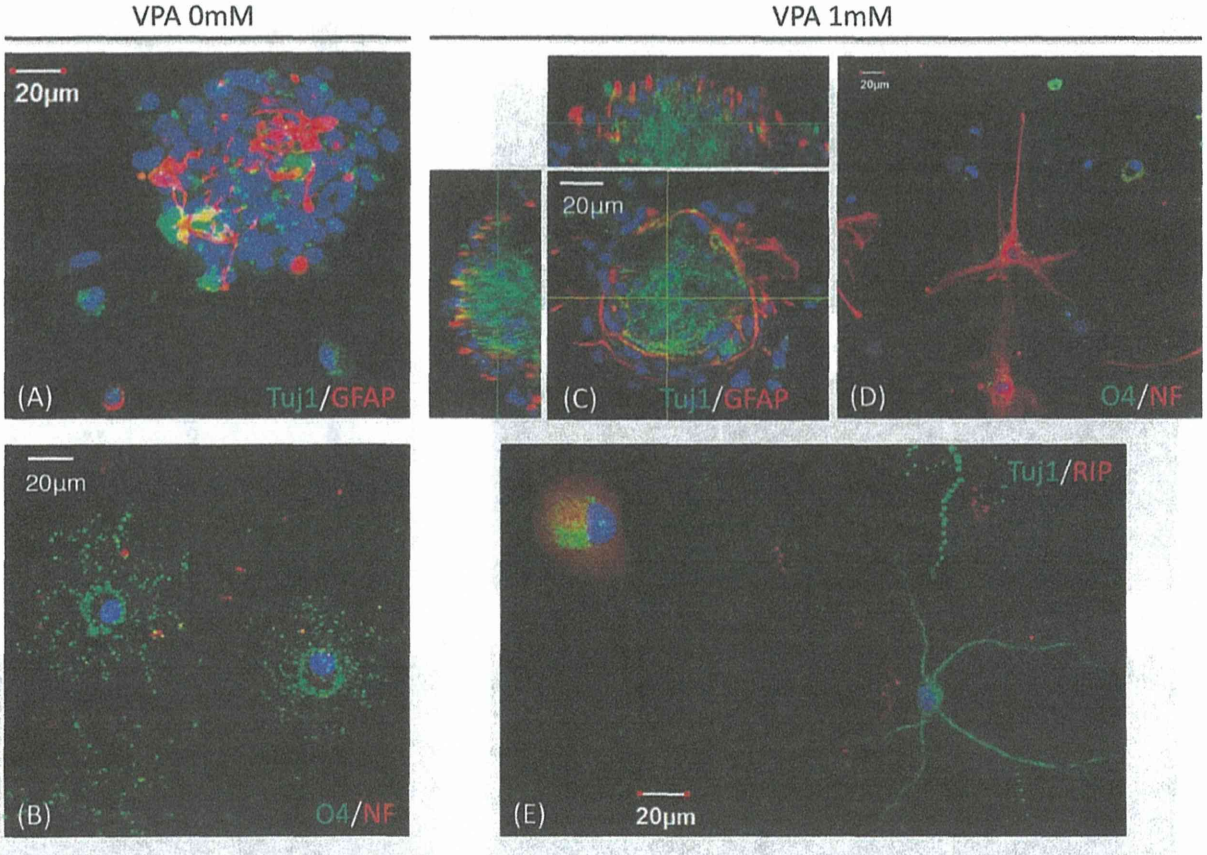


Fig. 2. Expression of cell-specific markers in adult rat OSCs treated with 0 mM (A,B) or 1 mM VPA (C–E). **A:** Coexpression of Tuj1 and GFAP in a subpopulation of 0 mM VPA-treated OSCs. **B:** O4-positive cells in 0 mM VPA-treated OSs exhibit almost no overlapping immunoreactivity with NF and display a branched morphology. **C:** In 1-mM VPA-treated OSCs, GFAP is rarely coexpressed with Tuj1. **D:** O4-positive cells in 1-mM VPA-treated OSs exhibit almost no overlapping immunoreactivity with NF. **E:** Tuj1-positive OSCs exhibit a typical neuronal soma and dendritic morphology; a subset of Tuj1-positive OSCs displays a round morphology and coexpresses RIP. Blue: DAPI-labeled nuclei. Scale bars = 20 μm. [Color figure can be viewed in the online issue, which is available at wileyonlinelibrary.com.]

0-, 0.3-, and 1-mM VPA treatment, respectively (Fig. 3A,B). These findings suggest a correlation between hyperacetylation of histones and OSC differentiation.

To examine the dedifferentiation effect of VPA, we investigated the gene and protein expression of nestin, an intermediate filament protein expressed in NSCs (Lendahl et al., 1990) and OSCs (Ben-Ari, 1985). We observed that the nestin expression levels were upregulated in OSCs treated with VPA (Fig. 3F). However, the number of nestin-positive cells was not significantly different between VPA-treated and control cultures (Fig. 3D,E).

Cell proliferation was estimated with BrdU, an analog of thymidine that is incorporated during DNA synthesis, which we have previously reported was observed in 6.7% ± 2.9% of OSCs (Ohnishi et al., 2013). In cultures treated with 1 mM VPA, BrdU uptake of OSCs decreased to 1.3% ± 0.9% (mean ± SD). These data suggest that OSCs treated with VPA did not exhibit stem cell-like properties brought on by dedifferentiation and were rather mostly terminally differentiated cells with distinct cell type characteristics. Therefore, we explored what classes of neurons VPA induced from OSCs.

## OSCs Differentiated Into GABA-Producing Neurons Following VPA Treatment

To determine the subtype of neurons derived from OSCs, we treated OSCs with VPA in culture and analyzed the neuronal subtypes by immunocytochemistry with antibodies specific for GABA and GAD67. VPA increased the number of GAD67- and GABA-positive OSCs as measured by immunofluorescence staining. Double-positive cells for Tuj1/GAD67 and Tuj1/GABA displayed typical neuronal soma and dendritic morphology (Fig. 4A). The percentage of GAD67-positive cells per Tuj1-positive cells was 0%, 46.1% ± 3.6%, and 54.3% ± 17.1% at 0-, 0.3-, and 1-mM VPA treatment, respectively (Fig. 4B). The percentage of GABA-positive cells per Tuj1-positive cells was 4.7% ± 8.2%, 29.4% ± 10.8%, and 27.2% ± 19.1% at 0-, 0.3-, and 1-

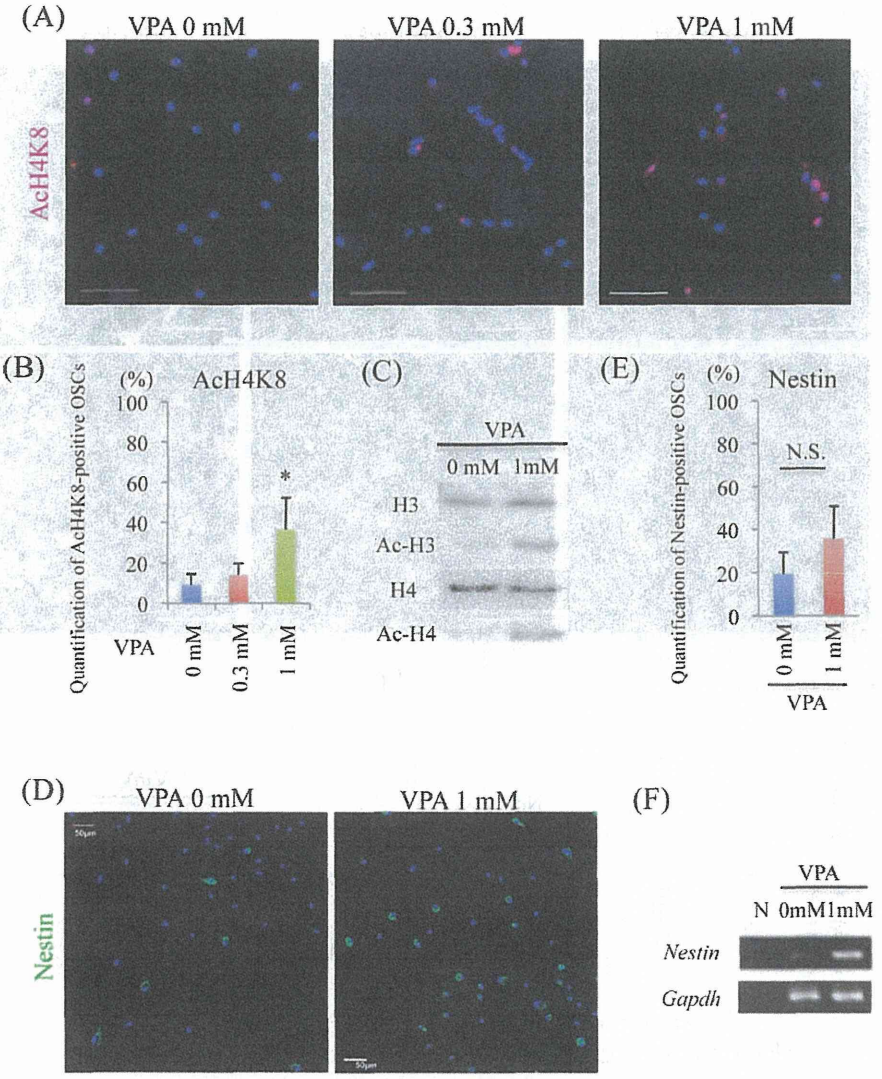


Fig. 3. Effect of VPA on OSC histone modification and nestin expression. **A:** Quantification of AcH4K8-positive OSCs. **B:** VPA increased the frequency of AcH4K8-positive OSCs. **C:** Western blot analyses show that cells treated with VPA had increased levels of acetylated histones H3 and H4. **D:** Quantification of nestin-positive OSCs. **E:** The number of nestin-positive cells was not significantly different with or without VPA. **F:** RT-PCR analysis shows that the expression of nestin is upregulated in OSCs treated with VPA. Error bars indicate SD. $*P < 0.05$. Scale bars = 50 μm. [Color figure can be viewed in the online issue, which is available at wileyonlinelibrary.com.]

mM VPA treatment, respectively. As further confirmation of these results, Western blot analysis revealed that the GAD67 proteins levels were also increased (Fig. 4C). These data strongly suggest that OSCs differentiated into GABA-producing neurons following VPA treatment in vitro.

### Grafted OSCs Differentiated Into GABA-Producing Neurons in TLE Model Rats

We next tested whether OSCs differentiate into GABA-producing neurons in vivo in the hippocampus of adult rats injected with KA to model TLE as the transplantation site. These rats exhibit inhibitory neuron loss, which contributes to seizure generation (Rao et al., 2006, 2007) and is similar to cell loss observed in patients with TLE. All rats exhibited stage 5 motor seizures, bilateral forelimb clonus with rearing and falling (Ben-Ari, 1985). Motor seizures were not apparent 12 hr after the onset of status epilepticus. Five days after seizure confirmation, we performed a hemilateral injection of EGFP-positive OSCs into the hippocampus. Cell suspensions (n = 6) and control medium (n = 4) were injected into the right and left sides, respectively. Rats were then given daily

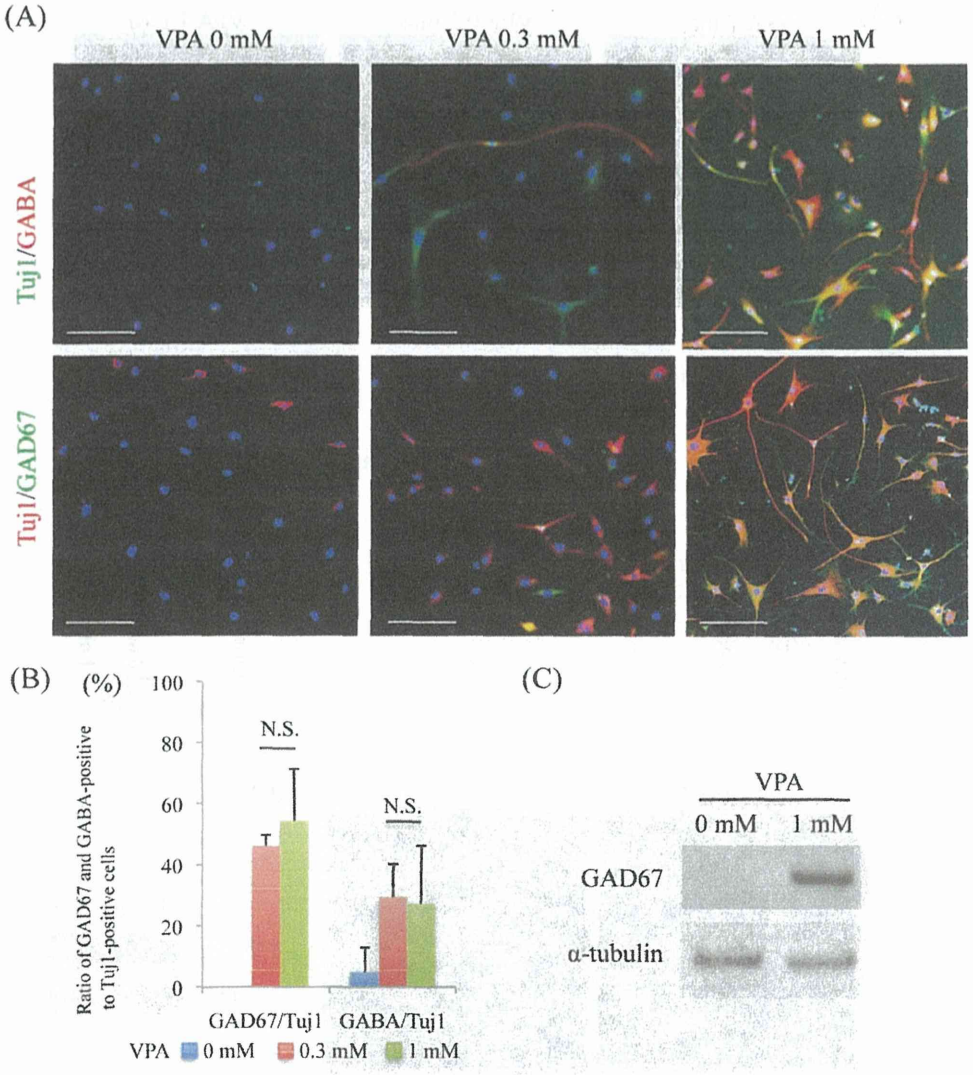


Fig. 4. OSCs differentiated into GABA-producing neurons following VPA treatment. **A:** Immunocytochemistry for GABAergic neuronal markers in OSCs cultured with 0, 0.3, or 1 mM VPA. **B:** Ratio of GAD67- and GABA-positive cells to Tuj1-positive cells cultured with 0, 0.3, or 1 mM VPA. **C:** Western blot analyses show that cells treated with VPA had increased levels of GAD67. Error bars indicate SD. Scale bars = 50 μm. [Color figure can be viewed in the online issue, which is available at wileyonlinelibrary.com.]

intraperitoneal injections of VPA or saline for 7 days, and tissues were examined 4 weeks posttransplantation.

To investigate the effect of VPA on the survival of grafted OSCs, we first analyzed sections by IHC with antibodies specific for GFP. Grafted cells were observed in the hippocampus and along fiber tracts (Fig. 5). GFP-positive cell counts in hippocampus of rats treated with ($n = 6$) or without ($n = 4$) VPA were $14.5 \pm 5.1$ and $22.4 \pm 11.4$, respectively. The survival rates of grafted cells with and without VPA were $10.8\% \pm 3.8\%$ and $16.8\% \pm 8.5\%$, respectively. These differences were not statistically significant.

To elucidate whether grafted OSCs differentiated into inhibitory neurons, we also investigated the expression Tuj1 and GAD67 in $GFP^+$ cells by IHC (Fig. 6). Double-positive cells for GFP/Tuj1 and GFP/GAD67 displayed neuronal morphology (Fig. 6), and far more GFP-labeled cells treated with VPA coexpressed GAD67 than in control animals ($66.2\% \pm 19.7\%$ vs. $6.2\% \pm 3.5\%$). In addition, $60.3\% \pm 24.6\%$ of GFP-labeled cells treated with VPA coexpressed calbindin vs. $2.5\% \pm 4.4\%$ in the absence of VPA.

To test the effect of transplanted OSCs on spontaneous seizures, we performed continuous EEG monitoring

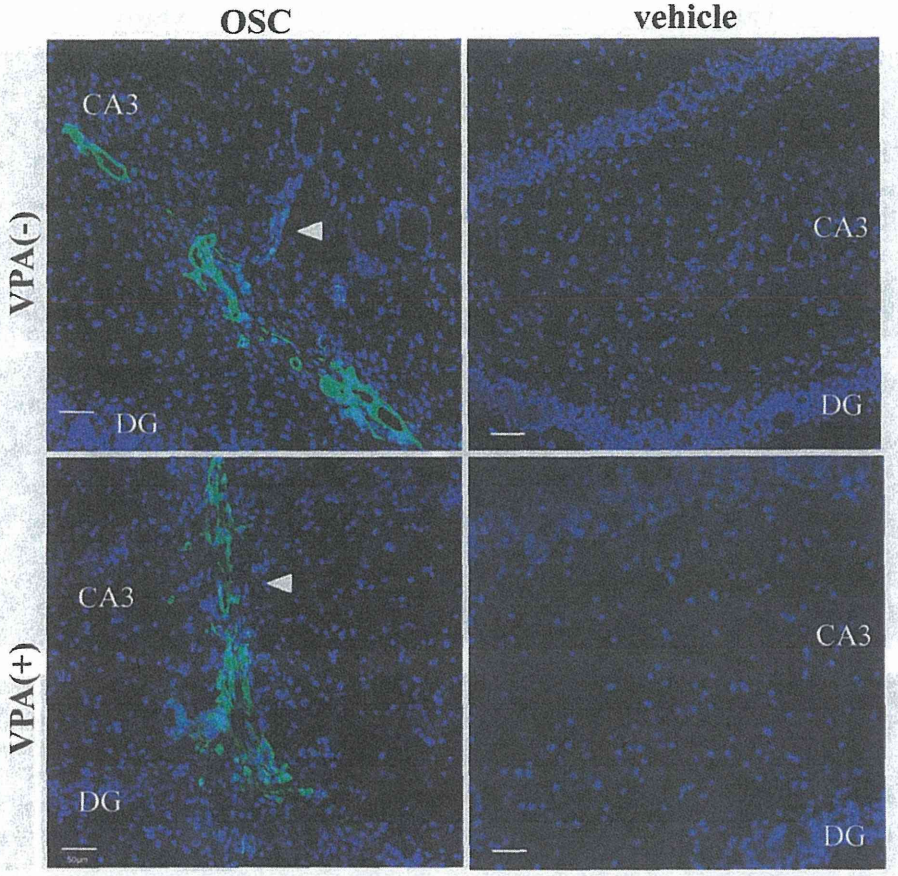


Fig. 5. Transplantation of OSCs into the hippocampus of TLE rats that were then given either VPA (n = 6) or PBS (n = 4). Photomicrographs of a coronal section show that grafted cells (green) were present in the hippocampus and along fiber tracts (arrowhead). There were no GFP-positive cells in vehicle-treated rats. Sections were labeled with DAPI (blue). DG, dentate gyrus; CA, cornu ammonis. Scale bars = 50 μm. [Color figure can be viewed in the online issue, which is available at wileyonlinelibrary.com.]

in the TLE model rats. Both the vehicle-treated and the OSC-transplanted hippocampi exhibited spontaneous electrographic seizures that were of a high frequency and voltage (Fig. 7). Then, to examine anticonvulsive effects of VPA, we determined the average numbers of epileptic spikes in the four experimental groups ($VPA^-/OSCs^-$, n = 3; $VPA^-/OSCs^+$, n = 3; $VPA^+/OSC^-$, n = 4; $VPA^+/OSCs^+$, n = 4). The average numbers of epileptic spikes were not significantly different among the groups (Fig. 7H), indicating that OSCs treated with VPA did not have an anticonvulsive effect and that grafted OSCs did not inhibit local epileptic activity. However, the ratio of spontaneous seizure spikes was significantly decreased in OSC-transplanted hippocampi compared with vehicle-treated hippocampi of VPA-administered rats at a ratio of 32.8% ± 15.3% vs. 1.2% ± 12.3%, respectively (Fig. 7I). Taken together with the IHC findings, these data suggest that grafted OSCs differentiated into GABA-producing inhibitory neurons.

## DISCUSSION

The results of the present study demonstrate that VPA promotes the differentiation of OSCs into GABA-producing neurons in vitro. In a rat model of TLE, OSCs differentiated into GABA-producing neurons following VPA treatment, but this did not lead to a significant reduction in the occurrence of electrographic epileptic spike. Thus, although OSCs represent a cell source for GABA-producing neurons that is readily modulated by VPA, we must more fully investigate the procedures used for transplantation, protocol for VPA treatment, and number of transplanted cells to determine whether OSCs are integrated into the host neural circuit and synaptically release GABA to inhibit neural activity and prevent seizures. Furthermore, this study did not examine whether other HDAC inhibitors and analogs had effects similar to those of VPA. Therefore, we could not directly ascribe the neuronal differentiation of OSCs to the HDAC-modulatory activity of VPA.

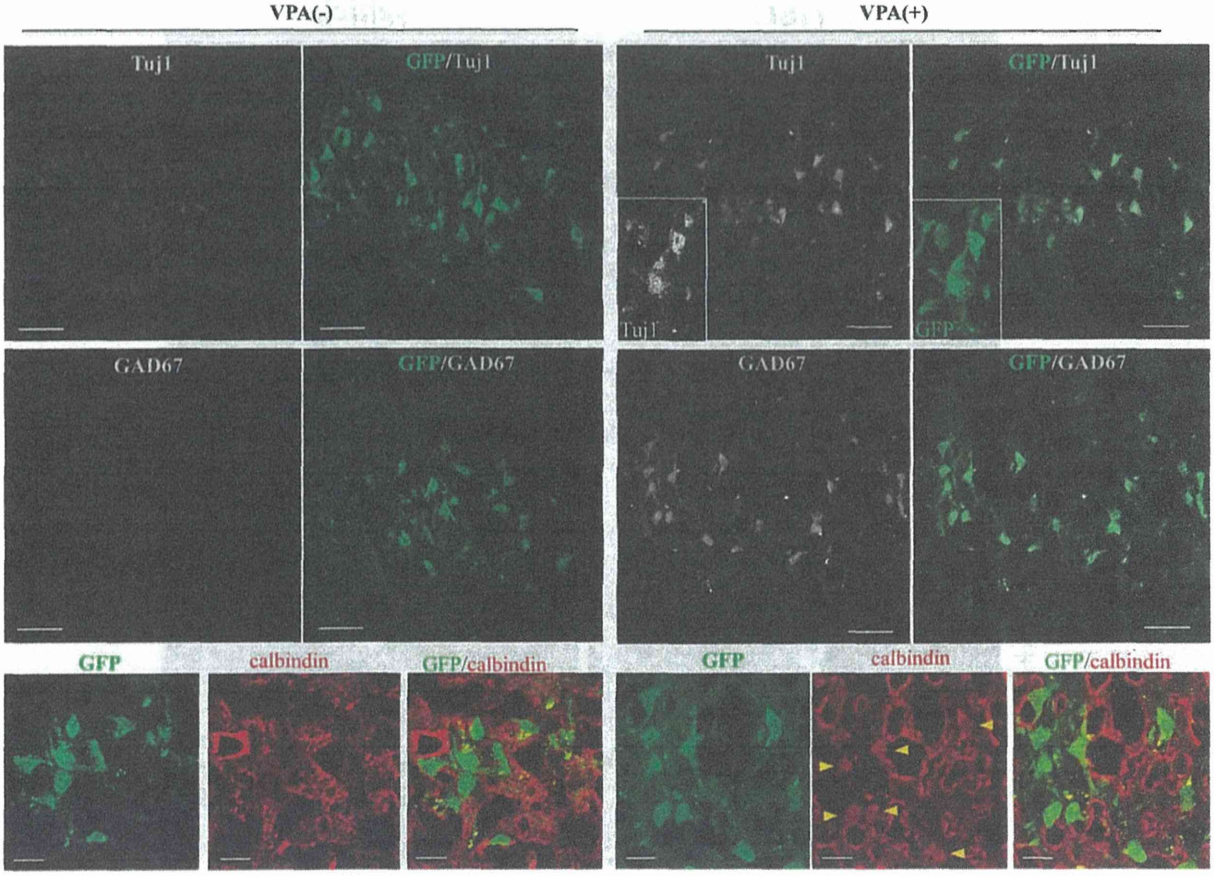


Fig. 6. Immunostaining for Tuj1 and GAD67 of OSCs in the hippocampus of TLE rats. GFP coexpressed with GAD67 and Tuj1 in VPA-administered rats. Single-plane images of cells at high magnification are provided in **insets**. GFP-positive cells rarely coexpressed GAD67 in non-VPA-administered rats. Grafted OSCs treated with VPA coexpressed calbindin (arrowheads). Scale bars = 50 μm in upper and middle row; 20 μm in lower row. [Color figure can be viewed in the online issue, which is available at wileyonlinelibrary.com.]

## VPA as a Regulator of GABA-Producing Neurons vs. Oligodendrocyte Cell Fate in OSCs

From previous studies showing that OPCs express the neural stem cell marker nestin and from VPA's role as an HDAC inhibitor, we hypothesize that VPA may function by respecifying OPC characteristics in OSCs to a neuronal fate through an HDAC-dependent mechanism. HDACs are necessary for oligodendrocyte differentiation and global chromatin remodeling, and histone acetylation induced by HDAC inhibitors is known to reverse lineage restriction partially. For instance, VPA has been shown to induce differentiation of adult hippocampal NSCs and embryonic forebrain neural progenitor cells through the inhibition of HDACs (Hsieh et al., 2004; Abematsu et al., 2010), and Laeng et al. (2004) demonstrated that VPA stimulates GABA neurogenesis from rat forebrain NPCs. Taken together, the current results indicate that VPA promotes differentiation of OSCs into inhibitory neurons, as observed in previous studies, but does not induce dedifferentiation into nestin-expressing NSCs. This observation might be explained by the activation of lineage-specific genes and silencing of "stemness" genes or activation of lineage-specific genes at greater levels than stemness genes.

## VPA-Modulated OSC Transplantation as a Therapeutic Strategy for Epilepsy

Several studies have focused on inhibitory interneuron transplantation as a treatment for neurological disease (Braz et al., 2012; Ma et al., 2012). The epileptic brain exhibits a pathological imbalance of excitation over inhibition. Cell replacement therapy is designed to restore normal levels of inhibition to seizure areas (Barry et al., 1987). Effective therapies require both the replacement of lost inhibitory cells and the restoration of neural circuits. Therefore, transplanted cells must disperse from the injection site, migrate into damaged areas, differentiate into

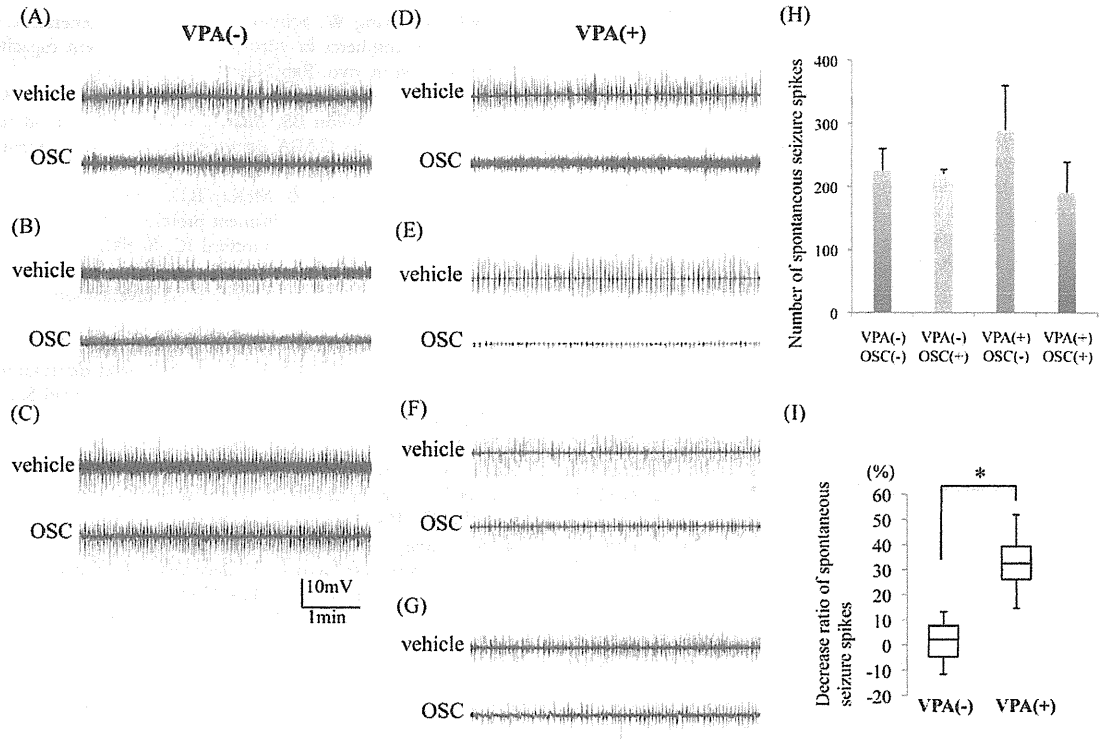


Fig. 7. Grafted OSCs reduce seizure occurrence in epileptic rats treated with VPA. **A–C:** Representative EEG recordings of spontaneous seizure in nontransplanted hippocampus (vehicle) and in hippocampus transplanted with OSCs in non-VPA-administered rats (n = 3). **D–G:** Representative EEG recordings of spontaneous seizure in nontransplanted hippocampus (vehicle) and in hippocampus transplanted with OSCs in VPA-administered rats (n = 4). **H:** Number of spontaneous seizure spikes. **I:** Boxplot shows the decrease ratio of spontaneous seizure spikes for each group based on continuous EEG recordings. $*P < 0.05$.

inhibitory interneurons, and be integrated into neural circuits. Thus, strategies to promote these properties in transplanted cells are of great interest.

Several cell sources have been evaluated for potential antiepileptogenic effects after transplantation into TLE model animals. The grafting of fetal hippocampal cells had an anticonvulsant effect and blocked seizure occurrence (Hattiangady and Shetty, 2012). Hunt et al. (2013) reported that inhibitory interneurons from the ganglionic eminence transplanted into the hippocampi of pilocarpine-treated mice prevented seizures.

### Therapeutic Levels of VPA Concentration

Serralta et al. (2006) reported that VPA concentrations, observed 30 min after intraperitoneal administration of 200 mg/kg VPA to rats, ranged from 120.3 to 570.9 μg/ml (mean 318.8 μg/ml) in serum, from 3.7 to 159.7 μg/ml (mean 25.8 μg/ml) in cerebrospinal fluid, from 78.6 to 260.9 μg/ml (mean 157.3 μg/ml) in the left hemisphere, from 74.5 to 340.9 μg/ml (mean 159.7 μg/ml) in the right hemisphere, and from 78.4 to 310.7 μg/ml (mean 158.2 μg/ml) in the brainstem. The permeability of the blood–brain barrier and cerebrospinal fluid synergistically contribute to the distribution of VPA in the brain. The current study used intraperitoneal administration of 150 mg/kg VPA to rats over 7 days. Accumulation of VPA and its active metabolites appeared to have an effect on grafted cells. We therefore assumed that we had attained the VPA concentration capable of inducing cellular differentiation in OSCs.

## CONCLUSIONS

Adult rat OSCs treated with VPA differentiated into GABA-producing neurons in vitro. Although grafted OSCs expressed Tuj1 and GAD67, the inhibitory effects of grafted OSCs proved insufficient for attenuating epileptic activity. These results suggest that OSCs are a VPA-modulated cell source for GABA-producing neurons. However, further investigation of their potential antiepileptic and other neuromodulatory properties is required before they can be adopted for clinical applications.

## ACKNOWLEDGMENTS

The authors thank Y. Eguchi for the generous provision of laboratory equipment, and Y. Takahashi for administrative assistance.

## CONFLICT OF INTEREST STATEMENT

The authors have no conflicts of interest.

## REFERENCES


Abematsu M, Tsujimura K, Yamano M, Saito M, Kohno K, Kohyama J, Namihira M, Komiya S, Nakashima K. 2010. Neurons derived from transplanted neural stem cells restore disrupted neuronal circuitry in a mouse model of spinal cord injury. J Clin Invest 120:3255–3266.

Balasubramaniyan V, Boddeke E, Bakels R, Kust B, Kooistra S, Veneman A, Copray S. 2006. Effects of histone deacetylation inhibition on neuronal differentiation of embryonic mouse neural stem cells. Neuroscience 143:939–951.

Barraud P, He X, Zhao C, Ibanez C, Raha-Chowdhury R, Caldwell MA, Franklin RJM. 2007. Contrasting effects of basic fibroblast growth factor and epidermal growth factor on mouse neonatal olfactory mucosa cells. Eur J Neurosci 26:3345–3357.

Barry DI, Kikvadze I, Brundin P, Bolwig TG, Bjorklund A, Lindvall O. 1987. Grafted noradrenergic neurons suppress seizure development in kindling-induced epilepsy. Proc Natl Acad Sci U S A 84:8712–8715.

Belachew S, Chittajallu R, Aguirre AA, Yuan X, Kirby M, Anderson S, Gallo V. 2003. Postnatal NG2 proteoglycan-expressing progenitor cells are intrinsically multipotent and generate functional neurons. J Cell Biol 161:169–186.

Ben-Ari Y. 1985. Limbic seizure and brain damage produced by kainic acid: mechanisms and relevance to human temporal lobe epilepsy. Neuroscience 14:375–403.

Braz JM, Sharif-Naeini R, Vogt D, Kriegstein A, Alvarez-Buylla A, Rubenstein JL, Basbaum AI. 2012. Forebrain GABAergic neuron precursors integrate into adult spinal cord and reduce injury-induced neuropathic pain. Neuron 74:663–675.

Conway GD, O'Bara MA, Vedia BH, Pol SU, Sim FJ. 2012. Histone deacetylase activity is required for human oligodendrocyte progenitor differentiation. Glia 60:1944–1953.

Fukuda H, Sano N, Muto S, Horikoshi M. 2006. Simple histone acetylation plays a complex role in the regulation of gene expression. Brief Funct Genomic Proteomic 5:190–208.

Gallo V, Armstrong RC. 1995. Developmental and growth factor-induced regulation of nestin in oligodendrocyte lineage cells. J Neurosci 15:394–406.

Gottlicher M, Minucci S, Zhu P, Kramer OH, Schimpf A, Giavara S, Sleeman JP, Lo Coco F, Nervi C, Pelicci PG, Heinzel T. 2001. Valproic acid defines a novel class of HDAC inhibitors inducing differentiation of transformed cells. EMBO J 20:6969–6978.

Gurvich N, Tsygankova OM, Meinkoth JL, Klein PS. 2004. Histone deacetylase is a target of valproic acid-mediated cellular differentiation. Cancer Res 64:1079–1086.

Hattiangady B, Shetty AK. 2012. Neural stem cell grafting counteracts hippocampal injury-mediated impairments in mood, memory, and neurogenesis. Stem Cells Transl Med 1:696–708.

Hsieh J, Nakashima K, Kuwabara T, Mejia E, Gage FH. 2004. Histone deacetylase inhibition-mediated neuronal differentiation of multipotent adult neural progenitor cells. Proc Natl Acad Sci U S A 101:16659–16664.

Hunt RF, Girskis KM, Rubenstein JL, Alvarez-Buylla A, Baraban SC. 2013. GABA progenitors grafted into the adult epileptic brain control seizures and abnormal behavior. Nat Neurosci 16:692–697.

Kondo T, Raff M. 2000. Oligodendrocyte precursor cells reprogrammed to become multipotential CNS stem cells. Science 289:1754–1757.

Krolewski RC, Jang W, Schwob JE. 2011. The generation of olfactory epithelial neurospheres in vitro predicts engraftment capacity following transplantation in vivo. Exp Neurol 229:308–323.

Laeng P, Pitts RL, Lemire AL, Drabik CE, Weiner A, Tang H, Thyagarajan R, Mallon BS, Altar CA. 2004. The mood stabilizer valproic acid stimulates GABA neurogenesis from rat forebrain stem cells. J Neurochem 91:238–251.

Lendahl U, Zimmerman LB, McKay RD. 1990. CNS stem cells express a new class of intermediate filament protein. Cell 60:585–595.

Lindsay SL, Johnstone SA, Mountford JC, Sheikh S, Allan DB, Clark L, Barnett SC. 2013. Human mesenchymal stem cells isolated from olfactory biopsies but not bone enhance CNS myelination in vitro. Glia 61:368–382.

Lyssiotis CA, Walker J, Wu C, Kondo T, Schultz PG, Wu X. 2007. Inhibition of histone deacetylase activity induces developmental plasticity in oligodendrocyte precursor cells. Proc Natl Acad Sci U S A 104:14982–14987.

Ma L, Hu B, Liu Y, Vermilyea SC, Liu H, Gao L, Sun Y, Zhang X, Zhang SC. 2012. Human embryonic stem cell-derived GABA neurons correct locomotion deficits in quinolinic acid-lesioned mice. Cell Stem Cell 10:455–464.

Marin-Husstege M, Muggironi M, Liu A, Casaccia-Bonnefil P. 2002. Histone deacetylase activity is necessary for oligodendrocyte lineage progression. J Neurosci 22:10333–10345.

Murdoch B, Roskams AJ. 2008. A novel embryonic nestin-expressing radial glia-like progenitor gives rise to zonally restricted olfactory and vomeronasal neurons. J Neurosci 28:4271–4282.

Murrell W, Feron F, Wetzig A, Cameron N, Splatt K, Bellette B, Bianco J, Perry C, Lee G, Mackay-Sim A. 2005. Multipotent stem cells from adult olfactory mucosa. Dev Dyn 233:496–515.

Ohnishi Y, Iwatsuki K, Shinzawa K, Ishihara M, Moriwaki T, Umegaki M, Kishima H, Yoshimine T. 2013. Adult olfactory sphere cells are a source of oligodendrocyte and Schwann cell progenitors. Stem Cell Res 11:1178–1190.

Othman M, Lu C, Klueber K, Winstead W, Roisen F. 2005. Clonal analysis of adult human olfactory neurosphere forming cells. Biotechnol Histochem 80:189–200.

Rao MS, Hattiangady B, Reddy DS, Shetty AK. 2006. Hippocampal neurodegeneration, spontaneous seizures, and mossy fiber sprouting in the F344 rat model of temporal lobe epilepsy. J Neurosci Res 83:1088–1105.

Rao MS, Hattiangady B, Rai KS, Shetty AK. 2007. Strategies for promoting antiseizure effects of hippocampal fetal cells grafted into the hippocampus of rats exhibiting chronic temporal lobe epilepsy. Neurobiol Dis 27:117–132.

Richardson WD, Young KM, Tripathi RB, McKenzie I. 2011. NG2-glia as multipotent neural stem cells: fact or fantasy? Neuron 70:661–673.

Serralta A, Barcia JA, Ortiz P, Durán C, Hernández ME, Alós M. 2006. Effect of intracerebroventricular continuous infusion of valproic acid versus single i.p. and i.c.v. injections in the amygdala kindling epilepsy model. Epilepsy Res 70:15–26.

Shechter D, Dormann HL, Allis CD, Hake SB. 2007. Extraction, purification, and analysis of histones. Nat Protoc 2:1445–1457.

Tome M, Lindsay SL, Riddell JS, Barnett SC. 2009. Identification of nonepithelial multipotent cells in the embryonic olfactory mucosa. Stem Cells 27:2196–2208.

Zhang X, Klueber KM, Guo Z, Lu C, Roisen FJ. 2004. Adult human olfactory neural progenitors cultured in defined medium. Exp Neurol 186:112–123.